JOURNAL OF CATALYSIS 125, 214–226 (1990)

The Influence of TiO_2 on the Speciation and Hydrogenation Activity of Co/Al_2O_3 Catalysts

MICHAEL A. STRANICK, MARWAN HOUALLA, AND DAVID M. HERCULES

Department of Chemistry, University of Pittsburgh, Pittsburgh, Pennsylvania 15260

Received February 7, 1989; revised April 2, 1990

The influence of TiO_2 on the distribution of supported species in 3 wt% Co/Al_2O_3 catalysts has been examined by X-ray diffraction, X-ray photoelectron spectroscopy (ESCA), Raman spectroscopy (LRS), and gravimetric analysis. The results show that for unmodified catalysts with low Ti loadings (<4 wt% Ti) the Co phase is present primarily as Co_3O_4 with lesser amounts of surface octahedral and tetrahedral cobalt [Co(o); Co(t)]. For catalysts having high Ti contents, Co_3O_4 formation is suppressed with increasing Ti loadings in favor of a $CoTiO_3$-like surface phase. Benzene and CO hydrogenation activity measurements indicate that Ti addition decreases the catalytic activity for both reactions. This has been attributed primarily to site blocking which results from the migration of reduced Ti species.

INTRODUCTION

It is well known that the nature of the carrier can have a dramatic influence on the surface structure and activity of supported metal catalysts (*1–5*). This is clearly illustrated by metals supported on reducible carriers or SMSI-type oxides (*6–11*). The dispersion of the supported metal, however, may vary with the type of carrier used. This often leads to ambiguity in discerning the role of the carrier from the effect of supported metal particle size. More conclusive results are obtained when SMSI-type oxides such as La_2O_3 and TiO_2 are used as "promoters" on high-surface-area supports such as Al_2O_3 or SiO_2 (*12–16*). In addition, the uniform deposition of a reducible carrier on a nonreducible support may permit systematic investigation of the SMSI effect.

Previous work from this laboratory has reported characterization of TiO_2 supported on γ-Al_2O_3 using X-ray photoelectron spectroscopy (ESCA or XPS), Raman spectroscopy, and X-ray diffraction (*17*). It was found that titania is well dispersed on alumina for Ti loadings below 14 wt%. The exclusive formation of a $TiO_2 : Al_2O_3$ surface phase occurred in the 1 to 6 wt% Ti loading range, with some anatase formation occurring at higher Ti loadings. The influence of TiO_2 on a 3% Co/Al_2O_3 catalyst was also reported (*17*). The dispersion of cobalt on titania-modified alumina carriers increased with increasing titania loading. The increase in cobalt dispersion was ascribed to formation of a surface cobalt phase to the detriment of Co_3O_4.

The present work describes the speciation of cobalt (fractions of Co_3O_4, tetrahedral Co^{+2} surface phase, and octahedral Co^{+2} surface phase) for a series of Co/Al_2O_3–TiO_2 catalysts using ESCA and gravimetric analysis. The surface structure of the Co/Al_2O_3–TiO_2 catalysts is compared with catalytic activity measurements for two reactions: CO hydrogenation, which has been reported to be structure sensitive (*18, 19*), and benzene hydrogenation, which is thought to be structure insensitive for cobalt catalysts (*20, 21*).

EXPERIMENTAL

Catalyst Preparation

Preparation of the TiO_2/Al_2O_3 carriers and 3% Co/Al_2O_3–/TiO_2 catalysts has been described in detail previously (*17*). The TiO_2-modified aluminas were prepared by non-

0021-9517/90 $3.00

aqueous pore volume impregnation of γ-Al_2O_3 using solutions of Ti(IV) isopropoxide, $Ti(O\text{–}iPr)_4$ (Aldrich Chemical Co.), dissolved in 2-propanol (J. T. Baker). Supports having TiO_2 loadings from 1 to 14 wt% as Ti were prepared. Cobalt was deposited on the TiO_2-modified aluminas by pore volume impregnation using cobalt nitrate (J. T. Baker) solutions. A constant loading of 3 wt% (of the alumina) as Co metal was employed. The TiO_2-modified aluminas and Co/Al_2O_3-TiO_2 catalysts were calcined in air for 6 h at 600 and 400°C, respectively.

Catalysts Characterization

Microbalance. The reduction/oxidation behavior of the titania-modified aluminas and Co/Al_2O_3–TiO_2 catalysts was studied using a Cahn 113 microbalance system. Prior to reduction, oxidic samples were dried at 400°C in ultrahigh purity 1% O_2/He (99.99% O_2, 99.999% He) until constant weight was achieved. Samples were then reduced in a flow of ultrahigh purity (99.999%) hydrogen at a temperature of 350°C for 12 h, followed by reoxidation at 400°C in O_2/He. The percentage of cobalt present as Co_3O_4 was calculated from the weight change measured during the reduction/reoxidation step relative to the weight change which would be expected assuming all cobalt was present as Co_3O_4. It has been shown (*30*) that Co_3O_4 is the only reducible phase present on Co/Al_2O_3 catalysts. Thus, the percent reduction reflects the percentage of Co_3O_4 in the oxidic catalyst.

X-ray photoelectron spectroscopy (ESCA or XPS). X-ray photoelectron spectra of reduced Co/Al_2O_3-TiO_2 catalysts were obtained with a Leybold–Heraeus LHS-10 spectrometer. The LHS-10 instrument is equipped with a reaction chamber bolted directly onto the analysis chamber of the spectrometer. Transfer of treated catalysts from the reactor to the analysis chamber is accomplished using a stainless-steel sample rod. The cobalt catalysts were mounted on the sample rod as pellets pressed at 2000 kg/cm^2. The ESCA Co/Al intensity ratios of catalyst pellets were identical to those of the corresponding powered samples, indicating that pressing pellets has no effect on the catalysts. Catalyst pellets were treated in the reaction chamber at 350°C in a 100 cm^3/min flow of ultrahigh purity (99.999%) hydrogen. The treated catalysts were then transferred directly to the spectrometer without exposure to air. The reaction chamber has been described in detail elsewhere (*22*). The LHS-10 instrument was interfaced to a Hewlett–Packard 1000 computer and was equipped with an aluminum anode (Al$K\alpha$ = 1486.6 eV) operated at 12 kV and 20 mA. ESCA spectra were recorded with the instrument operated in the fixed analyzer transmission mode. The residual pressure inside the spectrometer was 10^{-8} Torr or lower.

An AEI ES200 spectrometer was utilized to obtain ESCA spectra of sulfided catalysts. This permitted transfer of a treated catalyst from an external reaction chamber to the spectrometer, without exposure to air, using a sealable probe. The reaction chamber and sealable probe have been described in detail elsewhere (*23, 24*). Samples were mounted on the sealable probe as pellets pressed at 2000 kg/cm^2. Samples were sulfided in a flow of 15% H_2S/H_2 for 12 h at 400°C. The AEI instrument was interfaced to an Apple IIe microcomputer and was equipped with an aluminum anode operated at 12 kV and 20 mA. The residual pressure inside the spectrometer was 5×10^{-8} Torr.

It has been shown that the intensity ratio of supported phase and carrier ESCA peaks is related to the dispersion of the supported phase (*25–27*). In the present work the intensity ratios predicted for monolayer cobalt coverage were calculated using the model of Kerkhof and Moulijn (*27*). Photoelectron cross sections and escape depths used in theoretical calculations were obtained from Scofield (*28*) and Penn (*29*), respectively. The speciation of cobalt was determined from ESCA analysis of reduced and sulfided catalysts using a method which accounts for differences in dispersion of the

cobalt phases present on the catalyst surface (*30*). The Co metal/Al intensity ratios from the ESCA spectra of reduced catalysts were used to estimate the particle size of the metalic cobalt phase according to the method of Kerkhof and Moulijn (*27*). For cubic crystallites, the metal crystallite size is determined from the metal/support ESCA intensity ratio and the calculated metal/support intensity ratio for monolayer coverage according to

$$(I_m/I_s)_{crystallite}/(I_m/I_s)_{monolayer} = \lambda_m/C,$$

where λ_m and C are the photoelectron escape depth and crystallite size, respectively. This equation is valid for $C \gg \lambda_m$ (*27*).

Catalyst Activity

The benzene and CO hydrogenation activities of Co/Al_2O_3–TiO_2 catalysts were determined using a fixed-bed, flow microreactor operating under differential conditions. For benzene hydrogenation, benzene was introduced into a flow of ultrahigh purity hydrogen using a saturator maintained at 10°C. This provided a benzene partial pressure of 35 Torr in the reactant gas stream. Sodium metal was placed inside the saturator to remove traces of water and oxygen from the benzene. Activity measurements were made at a catalyst temperature of 70°C and used a 55 cm^3/min flow rate of reactant gas. Under these conditions the benzene conversion was below 4% for all catalysts studied. CO hydrogenation activity was determined at a catalyst temperature of 185°C and used a 25 cm^3/min flow of reactant gas, 3% CO/9% H_2/88% He. The flow rate of reactant gas was maintained with Matheson mass-flow controllers. Under these conditions the conversion of CO was below 4% for all catalysts studied.

For both reactions, products were separated using a Perkin–Elmer Sigma 2000 gas chromatograph and quantified using a Perkin–Elmer LCI 1000 integrator. For benzene hydrogenation the reaction product, cyclohexane, and unreacted benzene were separated using a column packed with a 10% Carbowax 400 on Chromosorb W-HP. In the case of CO hydrogenation, hydrocarbon products in the C_1–C_5 range were separated with an OV 101 column, while higher hydrocarbons were separated using a column packed with VZ10. Detection of reaction products was accomplished for benzene and CO hydrogenation using thermal conductivity and flame ionization detectors, respectively. Prior to exposure to the reactant gases, catalysts were activated by reduction in hydrogen at 350°C.

TABLE 1

Percentages of Reduction and Sulfidation for Co/Al_2O_3–TiO_2 Catalysts[a]

wt%	Ti/Al	% Reduction		% Sulfidation
		ESCA	Grav.	
0	0	64	62	77
1	0.011	67	57	81
2	0.021	66	64	83
4	0.041	56	53	81
6	0.066	50	44	86
8	0.087	40	30	84
10	0.11	33	28	84
14	0.15	26	20	85

[a] Percentages of reduction and sulfidation are ±10% rsd.

RESULTS

Characterization of Reduced Catalysts

Table 1 lists the percentage reduction of Co/Al_2O_3–TiO_2 catalysts as a function of Ti loading measured by ESCA (*30*). Ti had no effect on cobalt reducibility for catalysts with TiO_2 loadings of 2 wt% Ti (Ti/Al = 0.02) and below. Catalysts with TiO_2 loadings in excess of 2 wt% Ti exhibited a decrease from approximately 65 to 25% cobalt reducibility with increasing TiO_2 loading. The percentage reduction of the Co/Al_2O_3–TiO_2 catalysts determined gravimetrically is also shown in Table 1. Gravimetric measurements of percentage reduction are the same as those derived from ESCA measurements within experimental error.

Since Co_3O_4 is the only reducible cobalt

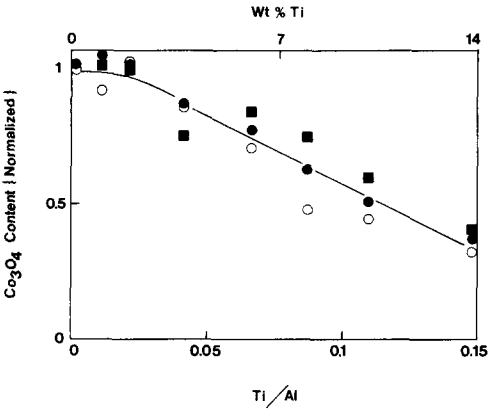

FIG. 1. Normalized Co_3O_4 content for 3% Co/Al_2O_3–TiO_2 catalysts. (●) Measured by ESCA; (○) measured by gravimetric analysis; (■) measured by Raman spectroscopy.

TABLE 2

ESCA Co $2p_{3/2}$/Al 2*s* Intensity Ratios for Oxidic, Reduced, and Sulfided Co/Al_2O_3–TiO_2 Catalysts[a]

Ti loading		ESCA Co/Al		
wt% Ti	Ti/Al	Oxidic	Reduced	Sulfided
0	0	0.35	0.34	0.24
1	0.011	0.34	0.31	0.24
2	0.021	0.34	0.35	0.23
4	0.041	0.45	0.41	0.33
6	0.066	0.49	0.45	0.43
8	0.087	0.52	0.53	0.44
10	0.11	0.61	0.57	0.46
14	0.15	0.68	0.69	0.52

[a] ESCA Co/Al intensity ratios are ±10% rsd or better.

phase on the catalysts at 350°C, then the percentage reduction reflects the percentage of Co_3O_4 in the oxidic precursor (*30*). Thus the percentage of Co_3O_4 is unaffected by the presence of TiO_2 for low TiO_2 loadings, while higher loadings of TiO_2 suppress Co_3O_4 formation. The amounts of Co_3O_4 on the Co/Al_2O_3–TiO_2 catalysts determined gravimetrically and by ESCA are consistent with those reported previously by Raman spectroscopy (*17*). This is illustrated in Fig. 1 where the percentages of Co_3O_4 for the Co/Al_2O_3–TiO_2 catalysts, normalized to the percentage of Co_3O_4 for the TiO_2-free catalyst, are plotted as a function of TiO_2 loading. Also, plotted versus TiO_2 loading in Fig. 1 are the intensities of the 693-cm^{-1} Co_3O_4 Raman band for the Co/Al_2O_3–TiO_2 catalysts, normalized to the Co_3O_4 band intensity of the TiO_2-free catalyst. It can be seen that the normalized Co_3O_4 Raman intensities are consistent with the normalized gravimetric and ESCA measurements of Co_3O_4 content. This indicates that changes in the Co_3O_4 Raman band intensity can be used to quantitatively measure changes in the Co_3O_4 content of low cobalt loading catalysts. There was no evidence by gravimetric analysis for reduction of the TiO_2 phase of the TiO_2/Al_2O_3 carriers treated in hydrogen at 350°C or by ESCA analysis of the reduced Co/Al_2O_3–TiO_2 catalysts. Reduction of titania would be indicated by the presence of an ESCA Ti $2p_{3/2}$ peak having a binding energy of approximately 457.5 eV, resulting from Ti^{+3} (*31*). A binding energy of 459.0 eV has been reported previously for Ti^{+4} (TiO_2) species (*17*). Reduction of the TiO_2 phase was also not observed by ESCA or gravimetric analysis following treatment of the TiO_2/Al_2O_3 carriers in hydrogen at 500°C. Similarly, no TiO_2 reduction was detected by ESCA following treatment of the catalysts in hydrogen at 500°C.

Table 2 presents the ESCA Co $2p_{3/2}$/Al 2*s* intensity ratios for the oxidic (*17*) and reduced Co/Al_2O_3–TiO_2 catalysts. It can be seen that the Co/Al intensity ratios of the reduced catalysts are unchanged (±5%) relative to those of the corresponding oxidic catalysts. The ESCA Ti 2*p*/Al 2*s* intensity ratios for oxidic (*17*) and reduced Co/Al_2O_3–TiO_2 catalysts are shown in Table 3. For corresponding titania loadings the Ti/Al intensity ratios of the reduced catalysts are also the same (±8%) as those of the oxidic catalysts. Thus, for catalysts having the same titania loading, hydrogen reduction at 350°C does not significantly alter either the cobalt or titania dispersion.

TABLE 3

ESCA Ti 2*p*/Al 2*s* Intensity Ratios for Oxidic, Reduced, and Sulfided Co/Al_2O_3–TiO_2 Catalysts[a]

Ti loading		ESCA Ti/Al		
wt% Ti	Ti/Al	Oxidic	Reduced	Sulfided
0	0	—	—	—
1	0.011	0.24	0.20	0.20
2	0.021	0.39	0.42	0.38
4	0.041	0.66	0.65	0.68
6	0.066	0.98	1.00	0.93
8	0.087	1.16	1.10	1.06
10	0.11	1.54	1.61	1.63
14	0.15	2.01	1.89	2.10

[a] ESCA Ti/Al intensity ratios are ±10% rsd or better.

TABLE 4

Crystallite Sizes Determined by ESCA and X-Ray Diffraction Line Broadening (XRDLB) for Reduced Co/Al_2O_3–TiO_2 Catalysts

Ti loading		Crystallite size (nm)[a]	
wt% Ti	Ti/Al	Co metal–ESCA[b]	Co_3O_4–XRDLB
0	0	7.8	7.6
1	0.011	8.2	7.3
2	0.021	8.2	7.3
4	0.041	8.3	7.0
6	0.066	7.5	6.2
8	0.087	7.0	5.8
10	0.11	6.4	*a*
14	0.15	5.6	*a*

Note. Co_3O_4 XRD peak not observed.

[a] Co metal and Co_3O_4 crystallite sizes are reproducible to within ±10%.

[b] Measured on reduced catalysts.

Cobalt Metal Particle Size

It has been reported that hydrogen chemisorption is an activated process for low cobalt loadings (*32*) and hence cannot be used to determine cobalt metal particle size. In addition, the stoichiometries for CO or oxygen chemisorption on cobalt are not known reliably (*32*), limiting the utility of these techniques. The cobalt metal particle size can be estimated from ESCA analysis of reduced catalysts using Co metal/Al intensity ratios and the method described by Kerkhof and Moulijn (*27*). Table 4 presents the mean crystallite size of the cobalt metal phase determined from ESCA analysis of reduced Co/Al_2O_3–TiO_2 catalysts. Titania has no influence on cobalt metal particle size for Ti loadings below 6 wt%, within experimental error. For catalysts having higher Ti loadings the cobalt metal particle size decreases, from approximately 8 to 6 nm, with increasing titania content.

The ESCA Co/Al intensity ratios shown in Table 2 are the same for the oxidic and reduced catalysts, suggesting no substantial change in cobalt dispersion following reduction. This is corroborated by Table 4 where the Co_3O_4 crystallite sizes of the oxidic Co/Al_2O_3–TiO_2 catalysts are presented. The Co_3O_4 crystallite sizes were determined from X-ray diffraction line broadening (XRDLB) using the Scherrer equation and correcting for instrumental broadening effects (*33*). Clearly, changes in Co_3O_4 crystallite size determined by XRDLB parallel those observed for the cobalt metal particle size determined by ESCA. For low Ti loadings, titania does not influence Co_3O_4 crystallite size, while a decrease in Co_3O_4 crystallite size is observed at higher titania loadings. The absence of XRD lines due to Co_3O_4 for the 10 and 14 wt% Ti catalysts precludes calculation of the crystallite size but suggests formation of Co_3O_4 crystallites smaller than ca. 5 nm and/or decrease in the fraction of Co phase present as Co_3O_4. The cobalt metal crystallite sizes were approximately 10% greater than the Co_3O_4 crystallites for corresponding titania loadings. This is well within the uncertainties associated with the Kerkhof and Moulijn method for particle size measurements by ESCA (e.g., assumptions of cubic crystallites, sheet-like structure of the support, homogeneous composition, etc.).

Characterization of Sulfided Catalysts

The percentage sulfidation for the Co/Al_2O_3–TiO_2 catalysts determined by ESCA

TABLE 5

Rates and Turnover Frequencies for CO and Benzene Hydrogenation

Ti loading		Rate		TOF	
wt% Ti	Ti/Al	Moles CO/h/g Co[a] $\times 10^3$	Moles C_6H_6/h/g Co[b] $\times 10^1$	Molecules CO/site/s $\times 10^4$	Molecules C_6H_6/site/s $\times 10^2$
0	0	7.2	2.5	9.5	3.3
1	0.011	6.8	2.4	9.5	3.3
2	0.021	4.8	1.8	6.7	2.5
4	0.041	2.6	1.0	3.7	1.4
6	0.066	1.7	0.39	2.2	0.50
8	0.087	1.1	0.31	1.3	0.37
10	0.11	1.0	0.072	1.1	0.078
14	0.15	1.0	0.034	0.95	0.032

[a] CO hydrogenation rates are ±15% rsd.
[b] Benzene hydrogenation rates are ±10% rsd.

using a previously described method (*30*) is shown in Table 1. The extent of cobalt sulfidation increased from 77% for the unmodified catalyst to approximately 83% for catalyst containing 2 wt% Ti. Titania loadings in excess of 2 wt% Ti did not affect the extent of cobalt sulfidation; an average of 83 ± 2% was observed. The ESCA Co/Al and Ti/Al intensity ratios for the sulfided Co/Al_2O_3–TiO_2 catalysts are presented in Tables 2 and 3, respectively. The Co/Al intensity ratios for the sulfided catalysts were approximately 20% lower than those for the corresponding oxidic catalysts. The lower intensity ratios for the sulfided catalysts indicate that sintering of cobalt occurs as a result of sulfidation. Covering of the cobalt phase by sulfur may also contribute to the decrease in Co/Al intensity ratios on sulfidation. The Ti/Al intensity ratios for the sulfided catalysts were the same (±8%) as those of the oxidic catalysts. Thus, titania dispersion is unaffected by treatment in H_2/H_2S.

Hydrogenation Activity

The steady-state rates of CO hydrogenation in moles CO/h/g metal are shown in Table 5 for the Co/Al_2O_3–TiO_2 catalysts. The CO hydrogenation rates are the averages of at least three measurements made after the catalysts had been on stream approximately 14 h and had reached steady-state activity. The CO hydrogenation rates decrease sharply with increasing TiO_2 loadings from approximately 0.0072 mol CO/h/g Co for the unmodified catalyst to 0.001 mol CO/h/g Co for catalysts having TiO_2 loadings of 8 wt% Ti and higher.

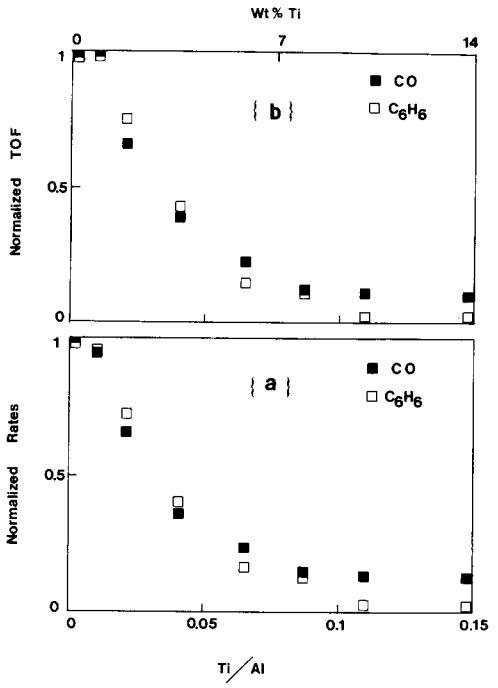

FIG. 2. CO and benzene hydrogenation activities for 3% Co/Al_2O_3–TiO_2 catalysts versus Ti loading. Data have been normalized to the activity of the unmodified catalyst. (a) Rates; (b) TOFs.

The rates of benzene hydrogenation in moles of C_6H_6/h/g of cobalt metal are also presented in Table 5. The rate of benzene hydrogenation decreased with increasing TiO_2 content from 0.25 for the unmodified catalyst to 0.01 mol C_6H_6/h/g/ Co metal for the 14 wt% Ti catalyst. Figure 2a shows the rates of CO and benzene hydrogenation normalized to the rates for the titania-free catalyst, plotted versus Ti loading. It can be seen that the decrease in activity relative to the unmodified catalyst follows the same trend for both CO and benzene hydrogenation.

Table 5 presents the turnover frequencies (TOF) for CO hydrogenation in molecules/site/s, for the Co/Al_2O_3–TiO_2 catalysts. The turnover frequencies were calculated using the rate data presented in Table 5 and an estimate of the number of active cobalt sites obtained from ESCA. The number of cobalt sites was estimated from the cobalt metal particle size (Table 4) assuming a spherical particle with 14.6 Co atoms/nm^2 (*32*). Figure 2b shows the variation of TOF for CO hydrogenation normalized to the TOF of the TiO_2-free catalyst, as a function of Ti loading. The TOFs for the Co/Al_2O_3–TiO_2 catalysts decrease with increasing TiO_2 loading in the same fashion as the rate per gram cobalt metal. Hence, the CO hydrogenation activity per cobalt site also decreases with increasing TiO_2 loading. Thus, it is evident that cobalt is less active for CO hydrogenation when supported on TiO_2-modified alumina, and the activity is lowest for catalysts having the highest amount of TiO_2.

The turnover frequencies for benzene hydrogenation in molecules of C_6H_6/site/s for the Co/Al_2O_3–TiO_2 catalysts are also presented in Table 5. The number of active cobalt sites also was estimated using the cobalt metal particle size determined by ESCA. It can be seen that the TOF for benzene hydrogenation also decreases sharply with increasing TiO_2 loading from 0.03 for the unmodified catalyst to 0.001 C_6H_6/site/s for the 14 wt% Ti catalyst. Thus, the benzene hydrogenation activity per site is decreased by the presence of titania. The plot of normalized TOFs for benzene hydrogenation versus Ti loading (Fig. 2b) showed behavior similar to the hydrogenation rate data of Fig. 2a.

TABLE 6

Distribution of Cobalt Species for Co/Al_2O_3–TiO_2 Catalysts

wt% Ti	Ti/Al	% Co_3O_4	% Co(t)[a]	% Co(o)[b] (total)	% Co(o)Al[c]	% Co(o)Ti[d]
0	0	64	23	13	13	0
1	0.011	67	19	14	12	2
2	0.021	66	17	17	10	7
4	0.041	56	19	25	8	17
6	0.066	50	14	36	5	31
8	0.087	40	16	44	3	41
10	0.11	33	16	51	0	51
14	0.15	26	15	59	0	59

[a] Co^{2+} in tetrahedral coordination.
[b] Total Co^{2+} in octahedral coordination.
[c] Co^{2+} in octahedral coordination formed through interaction with alumina.
[d] Co^{2+} in octahedral coordination formed through interaction with titania.

DISCUSSION

Surface Structure of Co/Al_2O_3–TiO_2 Catalysts

Characterization of the Ti-doped alumina carriers has been discussed in detail elsewhere (*17*). It was concluded from ESCA and Raman data that the TiO_2/Al_2O_3 carriers consisted primarily of a well-dispersed "surface" TiO_2 phase at all TiO_2 loadings (1 to 14 wt% Ti). For loadings greater than 6 wt% Ti, segregation of small amounts of anatase was observed by Raman spectroscopy. Large particles of anatase (particle size greater than ca. 4 nm) were observed by XRD only for the 14 wt% Ti support. The amount of anatase on the 8 and 10 wt% Ti-modified aluminas was below 1 wt% Ti (absolute); the modified alumina having 14 wt% Ti had approximately 2 wt% anatase (absolute).

The dispersion of cobalt increased with increasing TiO_2 loading for catalysts containing more than 2 wt% Ti. Co_3O_4 was detected on all catalysts by Raman spectroscopy; the intensity of the Co_3O_4 Raman bands decreasing with increasing Ti loading for loadings greater than 2 wt% Ti. Cobalt titanate was not detected by Raman on the oxidic Co/Al_2O_3–TiO_2 catalysts (*17*). Thus, Raman and ESCA data suggest that for TiO_2 loadings greater than 2 wt% Ti formation of a cobalt surface phase (Co^{2+} ions in octahedral and tetrahedral coordination within the support surface) occurs at the expense of Co_3O_4.

In the present work we have studied the distribution of cobalt species for the Co/

Al_2O_3–TiO_2 catalysts using an ESCA method outlined previously (*30*). Table 6 presents the percentage of Co present as Co_3O_4 as a function of Ti loading. Clearly the Co_3O_4 content was not affected by titania for low Ti loadings; high titania loadings caused a decrease in Co_3O_4 from approximately 65 to 26% with increasing TiO_2. The above results correlate well with the intensity decrease in the Co_3O_4 Raman bands and with gravimetric results. Thus, ESCA and gravimetric studies of reduced catalysts quantitatively confirm that modification of alumina by Ti suppresses Co_3O_4 formation in favor of a cobalt surface phase.

Table 6 also presents the percentages of octahedral [Co(o)] and tetrahedral [Co(t)] cobalt surface phase for the Co/Al_2O_3–TiO_2 catalysts determined by ESCA. It can be seen that the percentage of Co(t) decreases approximately 5% (absolute) at high titania loadings. For titania loadings above 2 wt% Ti, the percentage of Co(t) remains constant and averages 16 ± 2%. The percentage of Co(o) is unaffected by low Ti loadings but increases from approximately 15 to 59% (Table 6) with increasing Ti for loadings greater than 2 wt%.

The changes in cobalt species on the oxidic Co/Al_2O_3–TiO_2 catalysts can be rationalized by changes in the strength of interaction between cobalt and the modified support. The strength of the cobalt-carrier interaction determines whether cobalt will agglomerate during calcination, forming Co_3O_4, or will disperse across the support surface forming a cobalt surface phase. In the absence of titania or at low titania loadings most of the deposited cobalt interacts weakly with the carrier surface. Thus, cobalt agglomerates during calcination resulting primarily in formation of poorly dispersed Co_3O_4 and lesser amounts of Co(o) and Co(t). As the titania loading is increased, there is a greater quantity of surface titania with which the deposited cobalt can interact during calcination. The resulting cobalt–titania interaction inhibits agglomeration of cobalt during calcination (which predominates for low Ti loadings) in favor of dispersing cobalt across the support surface. This is evidenced by the decrease in Co_3O_4 and the increase in cobalt surface phase with increasing titania loading. Cobalt diffusion across the support surface also is responsible for the decrease in Co_3O_4 crystallite size and for the increase in cobalt dispersion with increasing titania loading.

The increase in cobalt surface phase for catalysts having titania loadings greater than 2 wt% Ti is due to an increase in Co(o) at the expense of Co_3O_4; the amount of Co(t) remains essentially constant. The constant amount of Co(t) reflects diffusion of cobalt into the alumina surface and the formation of a $CoAl_2O_4$-like surface spinel. As the titania loading is increased, the strong interaction between cobalt and titania results in an increase in Co(o) during calcination. It should be noted that $CoTiO_3$, in which Co^{2+} is octahedrally coordinated, was not detected on Co/Al_2O_3–TiO_2 catalysts by Raman spectroscopy (*17*). However, the interaction between the deposited cobalt and titania surface species during calcination could result in the formation of a Raman inactive $CoTiO_3$-like surface phase. The formation of this $CoTiO_3$-like surface phase would account for the increase in Co(o) with increasing titania loading. Thus, two forms of Co(o) are present on the surfaces of Co/Al_2O_3–TiO_2 catalysts: Co(o) formed through interaction with alumina, Co(o)Al, and that formed by interaction with the titania surface phase, Co(o)Ti. For the titania-free catalysts, formation of Co(o) can be due only to interaction with alumina and is therefore equal to Co(o)Al. By assuming that the percentage of Co(o)Al for the titania-modified catalysts decreases linearly with increasing titania coverage and that monolayer titania coverage occurs at approximately 10 wt% Ti (calculated based on the reaction of two surface hydroxyls per $Ti(O\text{–}iPr)_4$), the percentage of Co(o)Ti can be estimated. Thus, the percentage of Co(o)Ti is equal to the difference between the total Co(o) (Table 6) and the percentage of Co(o)Al. The percentage of Co(o)Al can be estimated by linearly extrapolating the percentage of Co(o)Al for

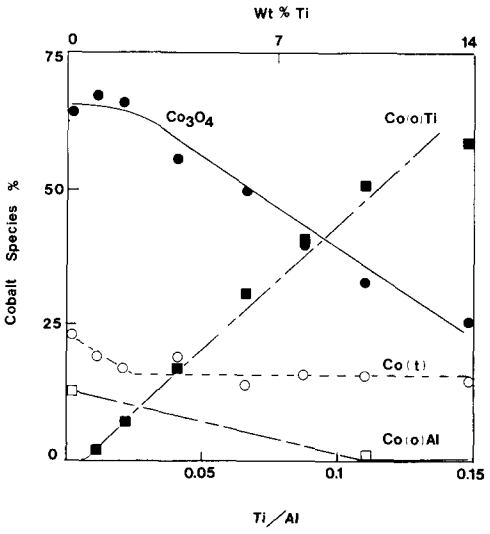

FIG. 3. Percentages of cobalt species for Co/Al_2O_3–TiO_2 catalysts versus Ti loading. (●) Co_3O_4; (□) Co(o)Al; (○) Co(t); (■) Co(o)Ti.

the unmodified catalyst (which equals the percentage of Co(o)) to 0% for the catalyst containing 10 wt% Ti. The percentages of Co(o)Al and Co(o)Ti calculated by this method for the Co/Al_2O_3–TiO_2 catalysts are presented in Table 6.

Figure 3 summarizes the distribution of cobalt species on the Co/Al_2O_3–TiO_2 catalysts, as a function of titania loading. For low titania loading catalysts, the percentage of Co_3O_4 is unaffected by titania. For titania loadings above 2 wt% Ti, the percentage of Co_3O_4 decreases with increasing titania loading. The decrease in the percentage of Co_3O_4 is accompanied by a comparable increase in the percentage of Co(o)Ti. This suggests that Co(o)Ti forms primarily at the expense of Co_3O_4. It is worth noting that this conclusion remains valid if one assumes that the percentage of Co(o)Al in Co/Al_2O_3–TiO_2 catalysts is invariant with TiO_2 coverage. The percentage of Co(t) decreases slightly for low titania loading catalysts and is invariant for higher titania contents. The small decline in Co(t) can be attributed to a decrease in the amount of alumina surface available for interaction with deposited cobalt due to coverage by titania. The constant percentage of Co(t) for Ti loadings greater than 2 wt% indicates that during calcination 16% of the deposited cobalt will diffuse into the alumina surface to form a $CoAl_2O_4$-like surface spinel. Thus, titania does not influence formation of Co(t) above loadings of approximately 2 wt% Ti. It should be noted that any attenuation of the Co(t) ESCA intensity by the TiO_2 surface layer will be insignificant within the experimental error of determinations.

Activity–Surface Structure Relationship

The activity of a supported metal catalyst for benzene and CO hydrogenation can be influenced by several different factors, including cobalt metal particle size, incomplete reduction of Co_3O_4, and migration of reduced TiO_x species. The activity of the Co/Al_2O_3–TiO_2 catalysts in the present study will be discussed in terms of these factors.

Benzene hydrogenation has been reported to be a structure-insensitive reaction (*20*) for cobalt catalysts, while CO hydrogenation is thought to be structure sensitive (*18, 19*). In the case of a structure-insensitive reaction, the turnover frequency should not be influenced by metal particle size (*21*). For a structure-sensitive reaction, changes in metal particle size result in changes in catalyst turnover frequency (*21*). Studies of the effect of particle size on benzene hydrogenation for cobalt catalysts have been limited, and the reported structure insensitivity of this reaction may be subject to question. Recent work on the hydrogenation of benzene using Ni/SiO_2 catalysts has suggested that metal particle size may influence catalyst activity for nickel particles in the 5- to 10-nm range (*34*). Others have reported essentially no effect of nickel particle size on benzene hydrogenation (*35, 36*). For CO hydrogenation, it has been reported that a decrease in cobalt metal particle size results in a decrease in the specific activity of cobalt supported on various oxide carriers (*32, 37*). A decrease in cobalt metal particle size has

also been used to rationalize the decrease in CO hydrogenation activity of Co/SiO_2 catalysts modified with titania (*19*).

The reducibility of the metal oxide phase of a supported metal catalyst can also influence catalyst activity. Indeed, recent results by Bartholomew and co-workers indicate that the apparent particle size dependence of CO hydrogenation activity can be attributed to changes in the extent of reduction of the metal phase (*38–39*). It has also been reported that the specific activity of nickel supported on various carriers is a function of the extent of nickel reduction (*40*). The greater the reduction of nickel, the higher the activity per nickel site. Unreduced nickel species act as a diluent toward the active nickel regions and can induce electron transfer from the metallic nickel to the unreduced surface phase. The changes in activity of nickel catalysts were attributed to these charge transfer effects (*40*). It has been argued by Ponec (*41*), however, that charge transfer from a reduced to an unreduced metal particle is negligible when compared to the total number of free electrons in a metal particle greater than 2 nm.

The migration of reduced TiO_2 species, TiO_x, onto active metal sites (SMSI effect) has been suggested as an explanation for the low benzene hydrogenation activity of several TiO_2-supported Group VIII metals, following reduction at temperatures above 300°C (*42–44*). These TiO_x species are thought to block active sites for benzene hydrogenation. It has been reported that the CO hydrogenation activities of Co/TiO_2 and Ni/TiO_2 catalysts (*3, 45*), as well as Pd/TiO_2 and Pd/SiO_2–TiO_2 catalysts (*12*), are higher than the corresponding Al_2O_3 or SiO_2 analogs. The higher activities of TiO_2 and SiO_2–TiO_2 supported catalysts were attributed to strong metal–support interaction (*3, 45*). Furthermore, it has been suggested that the presence of TiO_x moieties aids in the dissociation of CO (*12*). Studies of CO hydrogenation on Ni/TiO_2 catalysts, however, have reported a decrease in catalyst activity with increasing reduction temperature (*46*). It was suggested that TiO_x migration blocked CO hydrogenation sites for catalysts activated at temperatures greater than 350°C (*46*).

For the Co/Al_2O_3 catalysts in the present study, cobalt metal particle size and cobalt reducibility are influenced by modification of the support with TiO_2. Thus, changes in particle size and reducibility can influence the activity of the Co/Al_2O_3–TiO_2 catalysts for both CO and benzene hydrogenation. Partial reduction of TiO_2 and/or migration of TiO_x moieties onto metallic cobalt sites cannot be ruled out as factors which influence the activity of Co/Al_2O_3–TiO_2 catalysts. Reduction of TiO_2 was not observed by ESCA for either the Co/Al_2O_3–TiO_2 catalysts or TiO_2/Al_2O_3 carriers. There is approximately a 1.5-eV shift in the ESCA Ti $2p_{3/2}$ binding energy between Ti^{+4} and Ti^{+3}, determined from oxidation studies of a Ti metal foil (*31*). Computer synthesis of composite Ti $2p$ spectra for Ti^{+4} and Ti^{+3} using a FWHM of 2.7 eV and a 1.5-eV difference in binding energies showed that a minimum of 15% of the titania must be present as Ti^{+3} to be observed by ESCA.

The minimum weight change required for a reliable gravimetric determination of the extent of reduction is approximately 0.07 mg for the apparatus employed in this study. Smaller weight changes yield inaccurate extents of reduction because of the inherent difficulty in removing all of the water which forms during reduction. Thus, the determination of accurate extents of reduction by gravimetric analysis is limited by the ability to eliminate water from the catalyst sample. For a 50-mg sample of 10 wt% Ti/Al_2O_3, a 0.07-mg weight change corresponds to approximately 10% reduction of TiO_2 to Ti_2O_3. Treatment of the 10 wt% Ti/Al_2O_3 hydrogen at 350 or 500°C produced no discernable weight change. Thus, based on both gravimetric and ESCA estimates, if TiO_2 reduction is occurring, the extent of reduction must be less than 10%.

Interpretation of the CO and benzene hydrogenation activities in terms of the surface

structure for the Co/Al_2O_3–TiO_2 catalysts is simplified at low Ti loadings (1–4 wt%), where cobalt metal particle size and cobalt reducibility are not significantly influenced by titania. Thus, for low titania loadings, the decrease in CO and benzene hydrogenation activities cannot be readily explained by metal particle size effects and changes in cobalt reducibility. Migration of small quantities of TiO_x species onto metallic cobalt sites during catalyst activation can, however, account for the observed decrease. Decreases in activity with increased titania loading would result from blocking of a greater number of active cobalt metal sites by reduced titania species. For the Co/Al_2O_3–TiO_2 catalyst containing 4 wt% Ti, a significant decrease in catalyst activity was observed with no decrease in cobalt metal particle size and a limited change in the extent of reduction. The number of reduced titania species necessary to account for this decline in catalyst activity can be calculated, assuming that each cobalt metal site represents an active hydrogenation site and that an active site is blocked by one reduced titania species. The number of reduced titania species necessary to account for this decline in catalyst activity can be calculated, assuming that each cobalt metal site represents an active hydrogenation site and that an active site is blocked by one reduced titania species. The number of reduced titania species calculated from the decline in catalyst activity can then be used to estimate the extent of titania reduction. Following this approach, the decline in activity for the 4 wt% Ti catalyst can be accounted for by 4% reduction of titania, an extent below that which is detectable by ESCA or gravimetric analysis in the current study. Therefore, the absence of titania reduction seen by ESCA and gravimetric analysis does not preclude a titania reduction-site blocking mechanism to account for the observed decline in catalyst activity. In addition, it should be stressed that this estimated extent of titania reduction represents an upper limit since not all cobalt metal sites are necessarily catalytically active. Also, one reduced titania species may poison more than one active site. Site blocking by reduced titania species has been used to rationalize decreases in CO and benzene hydrogenation activities for several TiO_2-supported Group VIII metals (*42–44, 46*).

Site blocking by migration of small quantities of reduced TiO_2 species can account for the further decreases in CO and benzene hydrogenation activity at high Ti loadings. The interpretation of catalyst activity relative to the surface structure of the catalyst is complicated, however, by the fact that cobalt metal particle size and cobalt reducibility also decrease for high titania loadings. Both factors have been shown to influence the activity of supported metal catalysts (*18, 19, 32–40*). In addition, the fact that the decline in activity with increasing titania loading is not as great for high Ti loading catalysts as for low Ti loadings may be ascribed to poisoning of the most active sites with initial Ti addition and/or to less effective decoration of the metal particle for high Ti loadings (TiO_2 islands or discrete particles formation).

A model of the surface structure of the oxidic and activated Co/Al_2O_3–TiO_2 catalysts having titania loadings of 0, 4, and 10 wt% is presented in Fig. 4. For the unmodified catalyst, Co_3O_4, Co(t) and Co(o)Al are present on the surface of the oxidic catalyst. Following activation in hydrogen, the Co_3O_4 phase is reduced to Co metal, leaving the Co(t) and Co(o)Al phases unchanged. For the oxidic 4 wt% Ti catalyst, the titania surface phase and Co(o)Ti are present on the catalyst surface in addition to Co_3O_4, Co(t) and Co(o)Al. Activation in hydrogen of this catalyst again results in reduction of Co_3O_4 to cobalt metal, as well as reduction of a small amount (<10%) of titania surface phase. The reduced titania migrates onto the cobalt metal blocking active sites for hydrogenation. Not all active sites are blocked by titania as the catalyst exhibits activity for hydrogenation. In addition, both the amount and crystallite size of the cobalt

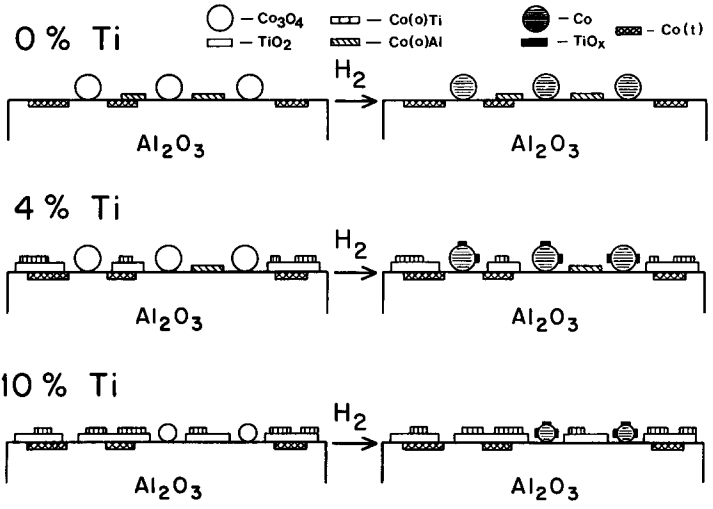

FIG. 4. Model of the surface structure of oxidic and activated Co/Al_2O_3–TiO_2 catalysts. Top, 0% Ti; middle, 4% Ti; bottom, 10% Ti.

metal phase are comparable to that for the titania-free catalyst. The Co(o)Al, Co(o)Ti, and Co(t) phases are unaffected by activation. For the oxidic 10 wt% Ti catalyst, titania surface phase, Co_3O_4, Co(t), and Co(o)Ti are present on the catalyst surface. The amount and crystallite size of Co_3O_4 have decreased relative to the unmodified and 4 wt% Ti catalysts. In addition, Co(o)Al is no longer present on the catalyst. Activation of the 10 wt% Ti catalyst results in the reduction of Co_3O_4 to cobalt metal, as well as reduction and migration of titania. A greater amount of titania is probably present on the cobalt metal surface, relative to the 4 wt% Ti catalyst, due to the greater availability of titania on the higher Ti loading catalyst. Thus, the hydrogenation activity of the 10 wt% Ti catalyst is further decreased. In addition, the particle size and amount of the cobalt metal are decreased relative to the 4 wt% Ti catalyst. This may contribute to the decline in catalyst activity.

CONCLUSIONS

1. The reducibility of 3 wt% Co/Al_2O_3–TiO_2 catalysts decreases with increasing Ti loading while the sulfidability remains unchanged. This is interpreted as a redistribution of cobalt species from Co_3O_4 and octahedral cobalt (+2) coordinated with alumina to a Co–titania interaction species, Co(o)Ti.

2. Cobalt metal particle size on the reduced catalysts is unaffected by Ti loading for catalysts containing less than 6% Ti. Above this, there is a decrease in cobalt particle size with Ti loading.

3. Benzene and CO hydrogenation rates and TOFs decrease with increasing Ti. For low Ti loadings, the decrease is attributed to a site-blocking mechanism resulting from migration of reduced TiO_2 species. Particle size changes and variation in the extent of Co reduction may also contribute to the decrease at high Ti loadings.

4. Raman spectroscopy can be used to monitor changes in the amount of Co_3O_4 present in Co–alumina catalysts. Raman results agree quantitatively with ESCA and gravimetric analysis.

ACKNOWLEDGMENTS

This work was supported, in part, by the U. S. Department of Energy under Grant DE-AC02-79ER10485. M. A. Stranick gratefully acknowledges the support of B. P. America in the form of a fellowship.

REFERENCES

1. Ng, K. Y. S., and Gulari, E., *J. Catal.* **92,** 340 (1985).
2. Ng, K. Y. S., and Gulari, E., *J. Catal.* **95,** 33 (1985).
3. Bartholomew, C. H., and Reuel, R. C., *J. Catal.* **85,** 78 (1984).
4. Bartholomew, C. H., and Vance, G. K., *J. Catal.* **91,** 78 (1985).
5. Vannice, M. A., Twu, C. C., and Moon, S. A., *J. Catal.* **79,** 70 (1983).
6. Tauster, S. J., Fung, S. L., and Garten, R. L., *J. Amer. Chem. Soc.* **100,** 170 (1978).
7. Tauster, S. J., and Fung, S. L., *J. Catal.* **55,** 29 (1978).
8. Resasco, D. E., and Haller, G. L., *J. Catal.* **82,** 279 (1983).
9. Simeons, A. J., Baker, R. T. K., Dwyer, D. J., Lund, C. R. F., and Madon, R. J., *J. Catal.* **86,** 359 (1984).
10. Ko, E. I., Hupp, J. M., Rogan, F. H., and Wagner, N. J., *J. Catal.* **84,** 85 (1983).
11. Singh, A. K., Pande, N. K., and Bell, A. T., *J. Catal.* **94,** 422 (1985).
12. Reick, J. S., and Bell, A. T., *J. Catal.* **99,** 278 (1986).
13. McVicker, G. B., and Ziemiak, J. J., *J. Catal.* **95,** 473 (1985).
14. Ko, E. I., Bafrali, R., Nuhfer, N. T., and Wagner, N. J., *J. Catal.* **95,** 260 (1985).
15. Murrell, L. L., and Yates, D. J. C., *Stud. Surf. Sci. Catal.* **7,** 1470 (1981).
16. Ko, E. I., and Wagner, N. J., *J. Chem. Soc. Chem. Commun.* **19,** 1274 (1984).
17. Stranick, M. A., Houalla, M., and Hercules, D. M., *J. Catal.* **106,** 362 (1987).
18. Bartholomew, C. H., and Fu, L., *J. Catal.* **92,** 376 (1985).
19. Lisitsyn, A. S., Golovin, A. V., Kuznetsov, V. L., and Yermakov, Y. I., *J. Catal.* **95,** 527 (1985).
20. Taylor, W. F., and Staffin, H. K., *J. Phys. Chem.* **71,** 3314 (1967).
21. Boudart, M., *in* "Proceedings, 6th International Congress on Catalysis, London, 1976" (G. C. Bond, P. B. Wells, and F. C. Tompkins, Eds.), Vol. 1, p. 1. Elsevier, Amsterdam, 1977.
22. Ledford, J. S., Houalla, M., and Hercules, D. M., to be published.
23. Patterson, T., Carver, J., Leyden, D., and Hercules, D. M., *J. Phys. Chem.* **80,** 1900 (1976).
24. Ng, K. and Hercules, D. M., *J. Phys. Chem.* **80,** 2094 (1976).
25. Defosse, C., Canesson, P., Rouxhet, P., and Delmon, B., *J. Catal.* **51,** 269 (1978).
26. Fung, S. C., *J. Catal.* **58,** 454 (1979).
27. Kerkhof, F. P. J. M., and Moulijn, J. A., *J. Phys. Chem.* **83,** 1612 (1979).
28. Scofield, J. H., *J. Electron Spectrosc. Relat. Phenom.* **8,** 129 (1976).
29. Penn, D. R., *J. Electron Spectrosc. Relat. Phenom.* **9,** 29 (1976).
30. Stranick, M. A., Houalla, M., and Hercules, D. M., *J. Catal.* **103,** 151 (1987).
31. Raupp, G. B., and Dumesic, J. A., *J. Phys. Chem.* **89,** 5249 (1985).
32. Reuel, R. C., and Bartholomew, C. H., *J. Catal.* **85,** 63 (1984).
33. Klug, H. P., and Alexander, L. E., *X-ray Diffraction Procedures,* p. 530. Wiley, New York, 1962.
34. Martin, G. A., and Dalmon, J. A., *J. Catal.* **75,** 233 (1982).
35. Nikolajenko, V., Bosacek, V., and Danes, V. L., *J. Catal.* **3,** 127 (1963).
36. Coenen, J. W. E., Schats, W. M. T. M., and van Meerten, R. Z. C., *Bull. Soc. Chim. Belg.* **88,** 435 (1979).
37. Lisitsyn, A. S., Kuznetsov, V. L., and Yermakov, Y. I., *Kinet. Katal.* **23,** 926 (1982).
38. Rameswaran, M., and Bartholomew, C. H., *J. Catal.* **117,** 218 (1988).
39. Bartholomew, C. H., Neubauer, L. R., and Lee, W. H., 11th North American Meeting of the Catalysis Society, PB15, 1989.
40. Turlier, P., Praliaud, H., Moral, P., Martin, G. A., and Dalmon, J. A., *Appl. Catal.* **19,** 287 (1985).
41. Ponec, V., *Stud. Surf. Sci. Catal.* **11,** 11 (1982).
42. Meriaudeau, P., Pommier, B., and Teichner, S. J., *Compt. Rend.* **C289,** 395 (1979).
43. Meriaudeau, P., Ellestad, H., and Naccache, C., *in* "Proceedings, 7th International Congress on Catalysis, Tokyo, 1980" (T. Seiyama and K. Tanabe, Eds.), p. 1464. Elsevier, Amsterdam, 1981.
44. Wang, I., Huang, W., and Wu, J., *Appl. Catal.* **18,** 273 (1985).
45. Vannice, M. A., and Garten, R. L., *J. Catal.* **56,** 236 (1979).
46. Burch, R., and Flambard, A. R., *J. Catal.* **78,** 389 (1982).